THE SPATIAL RESOLUTION CAPACITY OF HUMAN FOVEAL RETINA

Joy Hirsch and Christine A. Curcio

Yale University School of Medicine, Department of Ophthalmology and Visual Science,
310 Cedar Street BML 225, New Haven, CT 06510 and University of Washington School of Medicine,
Department of Biological Structure and the Department of Ophthalmology, Seattle,
WA 98195, U.S.A.

Abstract—An image on the retina of a human eye enters the visual system through an array of photoreceptors that sets the boundaries on the spatial detail available for neural representation. In order to investigate the extent to which the input spatial detail is preserved by the human neural system, we compare the anatomical spatial limits as determined by the Nyquist frequency, the highest spatial frequency reconstructable from the cone array, and measures of human acuity, the minimum angle resolvable. We find that the anatomical Nyquist limits determined along the temporal horizontal meridian of a well-studied human retina (Curcio, Sloan, Packer, Hendrickson & Kalina, 1987b) offer a reasonable prediction of human acuity within the retinal region extending from slightly off the exact foveal center to about 2.0 deg of retinal eccentricity. However, we find a narrow peak of anatomical resolution at the foveal center where the acuity appears to be overestimated by cone spacing.

Human photoreceptor lattice   Acuity   Retinal sampling   Anatomical resolution

INTRODUCTION

Foveal cone spacing is commonly assumed to be the basis of visual resolving power. Helmholtz reasoned that resolution of gratings consisting of light and dark bars required that at least one row of unstimulated cones associated with the dark bars lies between at least two rows of stimulated cones associated with the light bars (Helmholtz, 1911). The sampling theorem offers a more formal statement of this early hypothesis and states that an array of sensors cannot accurately reproduce an image with a spatial period that is less than half the center-to-center spacing between the sensors (Bracewell, 1965; Yellott, Wandell & Cornsweet, 1984). Although recent computational models of both human and machine vision require specification of this initial stage of visual processing (Poggio, Torre & Koch, 1985; Anderson & Van Essen, 1987), the human sampling mosaic based on retinal anatomy has not previously been described. Consequently, the limitations on spatial information based on the photoreceptor sampling and the limitations based on the postreceptoral neural substrate of the visual system have not been isolated. In this study we measure human cone center-to-center spacings in order to consider the hypothesis that foveal and near-foveal acuity is predicted by the retinal sampling grain.

METHODS

The human retina (H4 of Curcio et al., 1987b) was obtained from a 35-yr old male corneal transplant donor and fixed by immersion in mixed aldehydes. A retinal whole mount was prepared, cleared with dimethyl sulfoxide, and viewed with Nomarski differential interference contrast microscopy. Expansion of retinal area due to processing averaged 6% (3% linear) in a series of similarly prepared retinas (Curcio, Packer & Kalina, 1987a). Photomicrographs were taken at a focal plane corresponding to the presumed entrance aperture where the individual photoreceptor inner segments were just visible. This level was just vitread to the ellipsoid-myoid junction (Curcio, 1987).

Figure 1 shows the inner segments of the photoreceptor lattice in a strip extending $575\,\mu$m from the foveal center along the temporal horizontal meridian. At the beginning of the strip, top left, all profiles are cones. Rod profiles first appear at about $100\,\mu$m from the foveal center and are smaller than the cones. This figure illustrates a dramatic increase in cone cross sectional area and a decrease in cone density within the eccentricity range represented in the strip. The overall photoreceptor distribution in retina H4 resembles other previously described primate retinas (Østerberg, 1935;

Miller, 1979; Perry & Cowey, 1985; de Monasterio, McCrane, Newlander & Schein, 1985; Ahnelt, Kolb & Pflug, 1987; Hirsch & Miller, 1987; Schein, 1988), and the peak density of foveal cones is near the average for a group of young normal human eyes (Curcio et al., 1987b). The lattice strip is divided into 13 square windows each 48.87 μm on a side as indicated by the arrowheads in the figure. The exact foveal center is located by subdivision of the first two windows in Fig. 1 into eight equal subwindows each 23.94 μm on a side. The subwindow with the highest density is indicated by the brackets in Fig. 1. The temporal edge of that subwindow overlying the arrowhead at the top left of the figure was designated as 0.00 deg of retinal eccentricity. The spacings from each subsequent window in the strip were also assigned to the eccentricity of the temporal edge of the window. Angular eccentricity is given by $\tan^{-1} (d/F)$ where d is the measured retinal distance and F is the focal length (posterior nodal distance) of the eye which is assumed to be 16.67 mm as specified by the Gullstrand schematic human eye (Westheimer, 1972). Accordingly the angular scale is 291 μm/deg, and the retinal strip in this study extends from the foveal center to approx. 2.00 deg of eccentricity. An alternative schematic eye yields a conversion factor of 280 μm/deg which would increase the average center-to-center spacings reported here by about 3.5% and is within the estimated error of the means (Drasdo & Fowler, 1974).

RESULTS

In order to evaluate quantitatively the spatial detail preserved by the cone mosaic, the continuous retinal strip in Fig. 1 is converted to a series of dot matrices representing the centers of each cone. The mean spacing between nearest neighbors in each matrix is determined from the distribution of all pairwise center-to-center distances as described previously for similar analyses of monkey photoreceptor lattices (Hirsch & Hylton, 1984; Hirsch & Miller, 1987). Figure 2 confirms the subjective impression from Fig. 1 that the mean center-to-center cone spacing, d_{cc}, increases as a function of retinal eccentricity. These data are well described by the function $d_{cc} \mu m = 4.87 x^{0.22}$ for x greater than zero where x is retinal eccentricity in degrees of visual angle ($R^2 = 0.97$). Overall, the spacing increases by about a factor of about 2.5 within 2 deg of the foveal center. A similar retinal

topography has also been observed in other human and monkey retinas (Østerberg, 1935; Miller, 1979; Perry & Cowey, 1985; de Monasterio et al., 1985; Hirsch & Miller, 1987; Ahnelt et al., 1987; Schein, 1988).

This increase in cone spacing corresponds to a decrease in the anatomical resolving power of the lattice. According to the sampling theorem the highest anatomical resolving power (the Nyquist frequency) for a two-dimensional array is $2/\sqrt{3} (1/2d)$ cycles per degree (c/deg) where d is the center-to-center spacing of cones in degrees of visual angle (Bracewell, 1965; Snyder & Miller, 1977; Yellott et al., 1984). This calculation of the anatomical resolution limit assumes an ideal sampling array where (1) cones are equally spaced, and (2) the packing of cones is triangular.

However, as illustrated in Table 1, the actual human cone lattice only approximates this ideal lattice. For example, if the center-to-center spacings, d_{cc}, between the cones were actually equally spaced, the variation between nearest-neighbor distances would be vanishingly small. The actual average spacings (column 3) indicate that spacing uncertainty ranges from about 9 to 17% of the mean. Similarly, if the packing of cones were perfectly triangular, the angles between lines drawn from the center of any cone to the center of its nearest neighbor would not deviate from 60 deg of rotation (see Hirsch & Miller, 1987 for a detailed description of this procedure). The last column on Table 1 illustrates that the angular variation in center-to-center cone position deviates from 60 deg by as
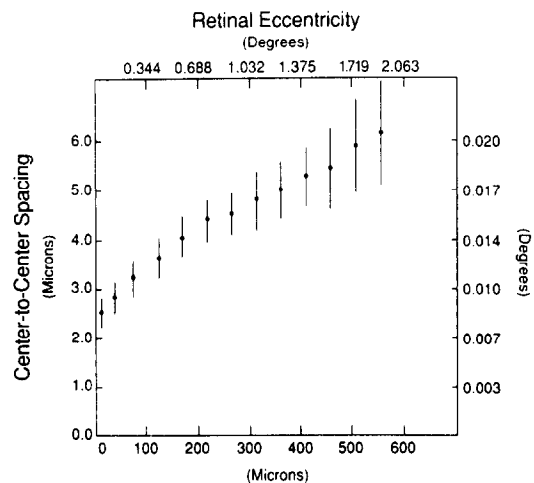

Fig. 2. Average center-to-center spacing of cones as a function of retinal eccentricity. Error bars represent ±1 SD in the spacings between all nearest neighbors. The retinal scale is 291 μm/deg of visual angle.
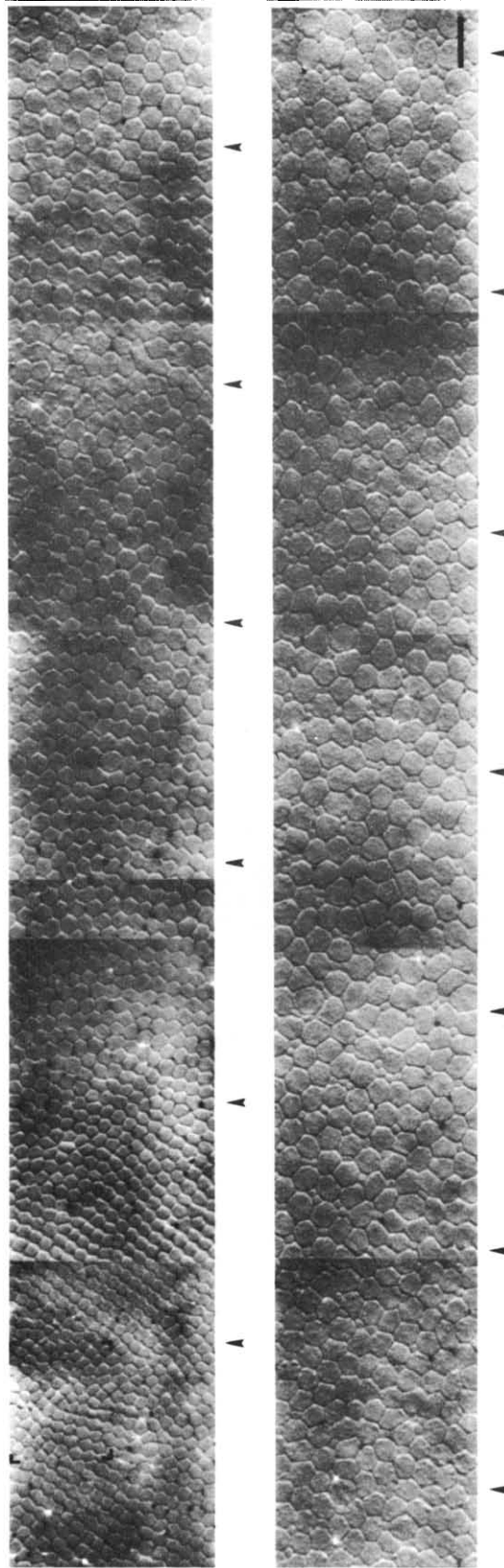
Fig. 1. Inner segments of a human foveal photoreceptor mosaic in a strip extending from the foveal center (indicated by the upper left arrow) along the temporal horizontal meridian. Arrowheads indicate the edges of the sampling windows. The large cells are cones and the small cells are rods. Brackets indicate a quadrant of the first sampling window with the highest density of cones. The midpoint of the boundary of this quadrant and a quadrant adjacent to it in the temporal direction (to the right) with similar density and mean spacing was considered to be the point of 0.0 eccentricity. The strip contains profiles of only cones up to the fifth window, where the small profiles of rods begin to intrude.

Bar = 10 μm

Table 1. Human cone lattice

Retinal region (deg)	Cone density (mm²)	Center-to-center spacing (mean ± SD)		Angle (mean ± SD) (deg)
		(μm)	(deg)	
0.00–0.08	183,283	2.53 ± 0.29	0.0087 ± 0.0010	58 ± 13
0.09–0.16	146,597	2.85 ± 0.31	0.0098 ± 0.0011	60 ± 11
0.17–0.33	113,897	3.24 ± 0.36	0.0112 ± 0.0013	60 ± 9
0.34–0.49	86,841	3.67 ± 0.40	0.0126 ± 0.0014	59 ± 8
0.50–0.66	68,513	4.08 ± 0.39	0.0140 ± 0.0014	59 ± 8
0.67–0.82	59,785	4.40 ± 0.44	0.0151 ± 0.0015	60 ± 9
0.83–0.99	54,985	4.54 ± 0.41	0.0156 ± 0.0014	60 ± 9
1.00–1.15	52,367	4.82 ± 0.60	0.0166 ± 0.0020	60 ± 12
1.16–1.32	44,948	5.02 ± 0.56	0.0173 ± 0.0019	64 ± 15
1.33–1.48	38,839	5.28 ± 0.60	0.0181 ± 0.0021	65 ± 16
1.49–1.65	37,966	5.45 ± 0.81	0.0187 ± 0.0028	64 ± 18
1.66–1.82	33,166	5.93 ± 0.97	0.0204 ± 0.0033	57 ± 15
1.83–1.98	32,729	6.16 ± 1.04	0.0213 ± 0.0036	55 ± 14

much as 14–25%. In view of the differences between the ideal and the actual lattice and the possibly (but not yet determined) deleterious effects of sampling disorder (French, Snyder & Stravanga, 1977; Yellott, 1983; Hirsch & Hylton, 1984; Hirsch & Miller, 1987), we consider that the Nyquist frequency yields an estimate of the maximum or best possible anatomical resolving power for each window. These "best case" Nyquist frequencies (the solid symbols in Fig. 3) show that the loss in anatomical resolving power is monotonic with retinal eccentricity and reaches a factor of about 2.5 by 2 deg from the foveal center.

In order to compare the resolution of the retinal sampling grain and the actual human acuity data, we plot the individual data (open symbols) from tasks using Snellen letters (Ludvigh, 1941); Landholt C (Sloan, 1968); and gratings (Weymouth, Hines, Acres, Raaf & Wheeler, 1928; Weiskrantz & Cowey, 1963; Westheimer, 1982). The criteria for selection of these resolution measures are (1) that the natural optics of the eye are used, (2) that the individual data are reported, and (3) that observers are experienced in order to assure that performance is optimal. These measures of human acuity are obtained by methods that determine the smallest feature identifiable including recognition (Snellen), location discrimination (Landholt C), and orientation discrimination (gratings). Each of these psychophysical measures require a less stringent set of image data than would be necessary for complete image reconstruction as specified by the sampling theorem. However, an

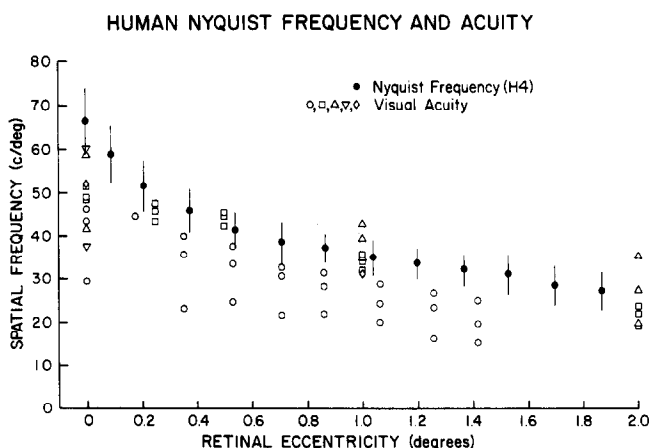HUMAN NYQUIST FREQUENCY AND ACUITY

Fig. 3. The Nyquist frequencies (solid symbols) for each retinal window are plotted as a function of retinal eccentricity in degrees. Error bars are based on the spread of the center-to-center spacing distributions of nearest neighbors. Open symbols include a representative set of previously reported measures of human visual resolution where (1) the optics of the eye were not bypassed (as in laser interferometry), (2) the individual data were reported, and (3) observers were experienced. Data are from Weymouth et al. (1928), (3 observers, gratings), O; Ludvigh (1941), (3 observers, Snellen), □; Wieskrantz and Cowey (1963), (3 observers, gratings), △; Sloan (1968), (1 observer, Landholt C), ◇; and Westheimer (1982), (2 observers, gratings), ▽.

alternative laser interferometric technique using a psychophysical measure of aliasing to determine the *effective* cone spacing in the foveal center provides corroborative estimates of foveal human acuity (Williams, 1985, 1986). These estimates range from 53 to 60 c/deg and fall within the range of the acuity measures presented in Fig. 3. Further, these estimates are also consistent with the laser interferometric measures of foveal acuity reported by Green (1970).

Inspection of Fig. 3 demonstrates that the best human acuity measures overlap the "best case" anatomical resolutions determined for this human cone lattice between about 0.2 and 2.0 deg of retinal eccentricity. Apparently, conventional resolution tasks can be performed at or near the "best case" limits based on cone sampling within this retinal region, even though a few observers tended to resolve below the calculated Nyquist frequencies for this lattice. Surprisingly, however, at the exact foveal center, acuity measures from *all* observers fell *below* the anatomical Nyquist frequencies suggesting that conventional resolution tasks in the fovea were not performed at the limits defined by cone sampling. At no eccentricity is the match between the anatomical and all the resolution data perfect, but it is "less good" in the foveal center.

DISCUSSION

Peak foveal cone densities in previously reported young adult retinas range from 100,000 to 300,000 cones/mm² (Østerberg, 1935; Miller, 1979; Yuodelis & Hendrickson, 1986; Ahnelt et al., 1987; Curcio et al., 1987b; Curcio, Sloan, Kalina & Hendrickson, 1989). Assuming that the packing of cones is approximately triangular, we can calculate a mean center-to-center foveal spacing based on the maximum cone density for these other eyes. If we also assume that all of the eyes within this range of reported densities have optical constants equal to the schematic eye used in this study (radial magnification factor = 291 μm/deg), we find that the Nyquist frequencies for this range of anatomical densities are approx. 50–86 c/deg, which still only partially overlaps the range of resolution acuities of approx. 30–60 deg. Furthermore, many peak densities fall between 150,000 and 300,000 cones/mm² (6 of 8 specimens from Curcio et al., 1989; Yuodelis & Hendrickson, 1986; Ahnelt et al., 1987), and the range of Nyquist limits for these high density

foveas is 61–86 c/deg using the same radial magnification factor. Thus, the likely mismatch of cone spacing and resolution acuity, as is seen for H4, is a potentially common occurrence.

The reasons for this probable foveal noncorrespondence between the anatomical and actual resolution are of particular interest. Calculations based on cone apertures show that it cannot be explained by signal integration over the optical apertures of cones (Miller & Bernard, 1983). The contrast of the sampled image is degraded relative to the source image because the sampled light is averaged across the apertures of the receptors. This contrast reduction, M, is given by:

$$M = 2J_1(\pi\gamma A)/(\pi\gamma A);$$

where J_1 is a Bessel function of the first kind, γ is spatial frequency, and A is the cone aperture. We determine the contrast reduction factor due to the presumed aperture size for retina H4 over a range of spatial frequencies extending to 200 c/deg, and find that contrast is reduced only by about 30–35% at the Nyquist frequencies determined from cone spacing. Therefore, demodulation due to aperture size cannot be the limiting factor.

Individual variability in foveal cone density cannot be conclusively ruled out as a source of noncorrespondence between anatomical and psychophysical resolution since the anatomical and psychophysical measures in this study are not from the same eyes. However, the sampling anatomy of this lattice and the psychophysical measures of acuity on other observers yield overlapping estimates of resolving power in retinal regions just off the foveal center, which illustrates a considerable lack of individual variability in the off-center regions. Since the only region of significant non-correspondence is on the foveal center, we consider the foveal divergence between the anatomical and psychophysical data to be a notable feature.

The conventional view that the retinal cone lattice is "matched" by the resolving power of the visual system is generally confirmed by these data for retinal regions slightly off the foveal center extending to about two degrees of retinal eccentricity. Since the natural optics of the eye were used in these measurements of acuity, it can also be concluded that the natural optics of the eye do not limit acuity over this region. However, at the foveal center of retina H4, the sampling theorem applied to cone spacing tends to *overestimate* the measured resolving power.

Thus these data raise the possibility that the "best case" anatomical resolution of the foveal lattice is not necessarily the critical limiting factor for foveal visual acuity, and that some potential spatial resolution in the foveal center may either be lost by the foveal optics or by the neural processing beyond the sampling stage.

REFERENCES

Ahnelt, P., Kolb, H. & Pflug, R. (1987) Identification of a subtype of cone photoreceptor, likely to be blue sensitive, in the human retina. *Journal of Comparative Neurology*, 255, 18–34.

Anderson, C. H. & Van Essen, D. C. (1987) Shifter circuits: A computational strategy for dynamic aspects of visual processing. *Proceedings of the National Academy of Science, U.S.A. 84*, 6297–6301.

Bracewell, R. M. (1965) *The Fourier transform and its applications* (pp. 189–218). New York: McGraw-Hill.

Curcio, C. A. (1987) Diameters of presumed cone apertures in human retina. *Journal of the Optical Society of America A, 4*, 70.

Curcio, C. A., Packer, O. & Kalina, R. E. (1987a) A whole mount method for sequential analysis of photoreceptor and ganglion cell topography in a single retina. *Vision Research, 27*, 9–15.

Curcio, C. A., Sloan, K. R., Packer, O., Hendrickson, A. E. & Kalina, R. E. (1987b) Distribution of cones in human and monkey retina. Individual variability and radial asymmetry. *Science, New York, 236*, 579–582.

Curcio, C. A., Sloan, K. R., Kalina, R. E. & Hendrickson, A. E. (1989) Human photoreceptor topography, submitted.

Drasdo, N. & Fowler, C. W. (1974) Non-linear projection of the retinal image in a wide angle schematic eye. *British Journal of Ophthalmology, 58*, 709.

French, A. S., Snyder, A. W. & Stavenga, D. G. (1977) Image degradation by an irregular retinal mosaic. *Biological Cybernetics, 27*, 229–233.

Green, D. C. (1970) Regional variations in the visual acuity for interference fringes on the retina. *Journal of Physiology, London, 207*, 351–356.

Helmholtz, H. (1911) In *Handbook der Physiologischen Optik*, Voss. Translated by Southall, J. P. C. (1924). *Helmholtz's treatise on physiological optics, Vol. II, the sensations of vision*. Optical Society of America.

Hirsch, J. & Hylton, R. (1984) Quality of the primate photoreceptor lattice and limits of spatial vision. *Vision Research, 24*, 347–356.

Hirsch, J. & Miller, W. H. (1987) Does cone positional disorder limit resolution? *Journal of the Optical Society of America A, 4*, 1481–1492.

Ludvigh, E. (1941) Extrafoveal visual acuity as measured by Snellen test letters. *American Journal of Ophthalmology, 24*, 303–310.

Miller, W. H. (1979) Ocular optical filtering. In Autrum H. (Ed.) *Handbook of sensory physiology* (VII, 6A). Berlin: Springer.

Miller, W. H. & Bernard, G. (1983) Averaging over the foveal receptor aperture curtails aliasing. *Vision Research, 23*, 1365–1369.

Østerberg, G. (1935) Topography of the layer of rods and cones in the human retina. *Acta Ophthalmologica* (Suppl.), 6, 1–103.

de Monasterio, F. M., McCrane, E. P., Newlander, J. K. & Schein, S. J. (1985) Density profile of blue-sensitive cones along the horizontal meridian of macaque retina. *Investigative Ophthalmology and Visual Science, 26*, 289–302.

Perry, V. H. and Cowey, A. (1985) The ganglion cell and cone distributions in the monkey's retina: Implications for central magnification factors. *Vision Research, 25*, 1795–1810.

Poggio, T., Torre, V. & Koch, C. (1985) Computational vision and regularization theory. *Nature, London, 317*, 314–319.

Schein, S. J. (1988) Anatomy of macaque fovea and spatial densities of neurons in foveal representation. *Journal of Comparative Neurology, 269*, 479–505.

Sloan, L. (1968) The photopic acuity-luminance function with special reference to parafoveal vision. *Vision Research, 8*, 901–911.

Snyder, A. W. & Miller, W. H. (1977) Photoreceptor diameter and spacing for highest resolving power. *Journal of Optical Society of America, 67*, 696–698.

Weiskrantz, L. & Cowey, A. (1963) Striate cortex lesions and visual acuity of the rhesus monkey. *Journal of Comparative and Physiological Psychology, 56*, 225–231.

Westheimer, G. (1972) Optical properties of vertebrate eyes. In Fourtes, M. G. F. (Ed.) *Handbook of sensory physiology* (VII/II, pp. 449–482). Berlin: Springer.

Westheimer, G. (1982) The spatial grain of the perifoveal visual field. *Vision Research, 22*, 157–162.

Weymouth, F. W., Hines, D. C., Acres, L. H., Raaf, J. E. & Wheeler, C. (1928) Visual acuity within the area centralis and its relation to eye movements and fixation. *American Journal of Ophthalmology, 11*, 947–960.

Williams, D. R. (1985) Aliasing in human foveal vision. *Vision Research, 25*, 195–205.

Williams, D. R. (1986) Seeing through the photoreceptor mosaic. *TINS, 9*, 193–198.

Yellott, J. I. Jr (1982) Spectral analysis of spatial sampling by photoreceptors: Topological disorder prevents aliasing. *Vision Research, 22*, 1205–1210.

Yellott, J. I. Jr (1983) Spectral consequences of photoreceptor sampling in the Rhesus Retina. *Science, New York, 221*, 382–385.

Yellott, J. I. Jr, Wandell, B. A. & Cornsweet, T. N. (1984) *Handbook of physiology* (Section I, pp. 257–316). Bethesda MD: American Physiology Society.

Yuodelis, C. & Hendrickson, A. (1986) A qualitative and quantitative analysis of the human fovea during development. *Vision Research, 26*, 847–855.